LANGMUIR Article
Cite This: Langmuir 2018, 34, 7509−7518
pubs.acs.org/Langmuir

Janus Liposomes: Gel-Assisted Formation and Bioaffinity-Directed Clustering

Mingming Wang,[†] Zening Liu,[†] and Wei Zhan*

Department of Chemistry and Biochemistry, Auburn University, Auburn, Alabama 36849, United States

Supporting Information

ABSTRACT: This article reports a high-yield procedure for preparing microsized (giant) Janus liposomes via gel-assisted lipid swelling and clustering behavior of these liposomes directed by biotin-avidin affinity binding. Confocal fluorescence microscopy reveals in detail that these new lipid colloidal particles display broken symmetry and heterogeneous surface chemistry similar to other types of Janus particles. An optimized formation procedure is presented, which reproducibly yields large liposome populations dominated by a single-domain configuration. This work further demonstrates that biotin-conjugated 1,2-dioleoyl-*sn*-glycero-3-phosphoethanolamine preferentially partitions into the liquid-disordered phase of the lipid matrix, rendering these Janus liposomes asymmetrical binding capacity toward avidin. This affinity binding drives irreversible and domain-specific cluster formation among Janus liposomes, whose structure and size are found to depend on the domain configuration of individual liposomes and incubation time.

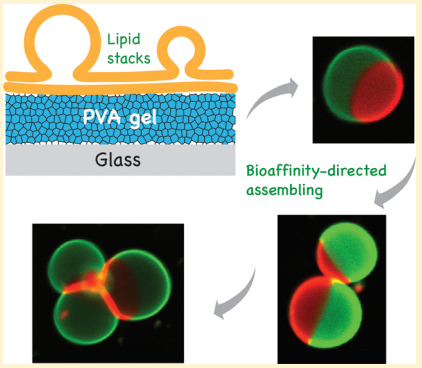

INTRODUCTION

This article reports a high-yield procedure for preparing microsized (giant) Janus liposomes via gel-assisted lipid swelling[1] and their clustering and aggregation behavior directed by biotin-avidin affinity binding. Similar to other types of Janus particles,[2−4] these lipid colloidal particles display broken symmetry and heterogeneous surface chemistry, whose formation is driven in this case by two closely related lipid-organizing mechanisms: hydrophobic mismatch[5,6] and cholesterol-induced liquid−liquid immiscibility[7,8] among lipids. Symmetrical liposomes bearing homogeneous surface composition have found widespread use in fundamental research[9−11] (e.g., cell biology, biophysics, and biotechnology) as well as in industry[12−14] (e.g., food, drug delivery, and cosmetics) ever since their discovery[15] in the 1960s. By contrast, relatively little work has been done so far on Janus liposomes, their characteristics and application potential yet to be fully examined.

Much research has been devoted lately to micro- and nanoparticles carrying broken symmetry and heterogeneous surface chemistry, i.e., patchy particles,[16,17] whose structural complexity and high information content offer exciting new opportunities for creative design of functional materials. Janus particles, with two opposing halves of distinct makeup/functionality, represent the simplest patchy particle system and thus a natural place to start an investigation. Indeed, recent studies on Janus particles have already uncovered several unique features, which their symmetrical counterparts do not possess. For example, Janus particles equipped with asymmetrical interfacial characteristics and anisotropic binding capacity can self-assemble into higher-order hierarchical structures, such as clusters[18] and microcapsules.[19] Moreover, Janus particles decorated with physically responsive or (bio)chemically reactive functionalities have been tested as micro- and nanosized motors,[20,21] which can overcome Brownian motion in fluids in response to specific external stimuli. As the number of efficient and precise particle synthesis methods continues to grow, so will the level of sophistication in their applications.

Janus liposomes in principle share many of the same promises, whose realization first of all calls for a robust method to make such colloidal particles. Ideally, this method should enable (1) precise and tunable control of liposomes' asymmetry and heterogeneity and (2) high-yield and reproducible liposome production generally applicable to many types of lipids. In search of such a method, we have found a reliable approach based on gel-assisted formation of phase-separated giant liposomes. Here, phase separation introduces heterogeneity to the liposomes, essentially adding another degree of freedom to the system. Interfacing lipids with dry and inert hydrogels, such as poly(vinyl alcohol) (PVA),[1] on the other hand, sets up an important mechanism for constant lipid hydration and liposome detachment, improving the overall yield.

Lateral phase separation in lipid monolayers and bilayers is of fundamental importance to our understanding in the organization and functions of cell membranes and hence has long been a key area of research in membrane biophysics.[22−24] A lasting focus in this area has been cholesterol-induced liquid−liquid immiscibility,[7,8] which occurs when cholesterol is mixed

Received: March 10, 2018
Revised: May 4, 2018
Published: May 31, 2018

Downloaded via AUBURN UNIV on July 5, 2018 at 18:52:42 (UTC).
See https://pubs.acs.org/sharingguidelines for options on how to legitimately share published articles.

© 2018 American Chemical Society

DOI: 10.1021/acs.langmuir.8b00798
Langmuir 2018, 34, 7509−7518

with phospholipids or sphingolipids with saturated/unsaturated hydrocarbon chains, for example, 1,2-dipalmitoyl-*sn*-glycero-3-phosphocholine (DPPC) and 1,2-dioleoyl-*sn*-glycero-3-phosphocholine (DOPC). Such immiscibility can be readily followed by fluorescence microscopy,[25−27] in which individual giant liposomes of this ternary system can be found to display disparate surface patterns, e.g., circular domains, when labeled with phase-selective dyes. This lateral phase segregation results primarily from combined effects due to (1) hydrophobic mismatch[5,6] between DPPC and DOPC and (2) preferential association of the structurally rigid cholesterol with DPPC, which produces a liquid-ordered (l_o) phase enriched with DPPC and cholesterol and a liquid-disordered (l_d) phase comprising mainly DOPC.[7,8] Besides fluorescence microscopy, NMR has proved to be another essential tool in the characterization of lipid-phase separation. By systematically varying the lipid mixing ratios and monitoring the quadrupolar splitting in ^{2}H NMR spectra, for example, detailed phase diagrams of the DPPC/DOPC/cholesterol system have been constructed by Keller,[28,29] Davis,[30,31] and their co-workers. Quantitative description of model lipid systems such as this not only provides us an essential window to look into the baseline protein-free biomembrane thermodynamics and associated critical phenomena, but also offers opportunities for development of new lipid-based biomaterials.

Taking advantage of these findings, Beales, Nam, and Vanderlick carried out the first systematic study[32] on giant Janus liposomes electroformed from DPPC/DOPC/cholesterol in 2011. Using lipid-phase separation to guide DNA anchoring on these liposomes, furthermore, they successfully rendered these Janus liposomes asymmetrical binding ability, which preferentially occurs via liquid-ordered domains. Mixing such Janus liposomes carrying complementary DNA strands then led to the formation of various size-limited liposome clusters, a unique behavior not displayed by homogeneous single-domain liposomes. This work clearly demonstrates the possibility to prepare Janus particles using lipids and moreover, unique features of liposomes as a colloidal material, e.g., their deformable surfaces.

We report herein a new procedure to prepare microsized Janus liposomes via gel-assisted lipid swelling and a straightforward strategy to impart asymmetrical reactivity on these liposomes using biotin-avidin affinity binding. This procedure not only reproducibly yields large liposome populations that can be harvested for later uses, but also enables control over liposome's domain configuration. We further show that biotin-conjugated 1,2-dioleoyl-*sn*-glycero-3-phosphoethanolamine (biotin-DOPE) preferentially partitions into the liquid-disordered phase of the lipid matrix, rendering these Janus liposomes asymmetrical binding capacity toward avidin. Finally, we find that such affinity binding drives irreversible and domain-specific cluster formation among Janus liposomes, whose structure and size depend on the domain configuration of individual liposomes and incubation time.

EXPERIMENTAL SECTION

Reagents. All lipids, including 1,2-dipalmitoyl-*sn*-glycero-3-phosphocholine (DPPC), 1,2-dioleoyl-*sn*-glycero-3-phosphocholine (DOPC), 1,2-dioleoyl-*sn*-glycero-3-phosphoethanolamine-*N*-(biotinyl) (sodium salt) (biotin-DOPE), 1,2-dioleoyl-*sn*-glycero-3-phosphoethanolamine-*N*-(cap biotinyl) (sodium salt) (biotin-cap-DOPE), 1,2-dipalmitoyl-*sn*-glycero-3-phosphoethanolamine-*N*-(cap biotinyl) (sodium salt) (biotin-cap-DPPE), 1,2-dioleoyl-*sn*-glycero-3-phosphoethanolamine-*N*-(lissamine rhodamine B sulfonyl) (ammonium salt) (rho-DOPE), and 23-(dipyrrometheneboron difluoride)-24-norcholesterol (Bodipy-chol), were products of Avanti Polar Lipids (Alabaster, AL). Other chemicals, including poly(vinyl alcohol) (PVA, MW: 89 000−98 000 and 145 000), cholesterol, NeutrAvidin biotin-binding protein, and Alexa Fluor 488-conjugated avidin, were obtained from Sigma-Aldrich. Deionized (DI) water of 18.2 MΩ·cm (Millipore) was used throughout this work.

Liposome Preparation. Janus as well as symmetrical giant liposomes of desired compositions were prepared by following the gel-assisted lipid swelling method reported by Marques and co-workers[1] with minor modifications. In the sequence of operation, specifically, our procedure can be broken down into four steps. (1) Material/substrate preparation, which includes poly(vinyl alcohol) (PVA) solution, glass substrates, and lipid precursor solutions. The PVA aqueous solution used in this procedure contains 5 wt % polymer, which is dissolved by continuously stirring the polymer in DI water maintained at 80 °C, whereas the glass slides (VWR, 1 × 1 in, 1 mm thickness) are cleaned by sonication in acetone, DI water, dilute detergent aqueous solutions, and DI water again and then blow-dried by a nitrogen stream. All lipid precursors used in this work are prepared in chloroform with total lipid concentration of 5 mM, and their compositions are specified in the main text. (2) PVA gel preparation, which is done by first evenly spreading 100 μL of the PVA solution on a precleaned glass slide at room temperature and then drying it on a hot plate at 50 °C for 0.5 h. (3) Lipid deposition on PVA gel. To achieve this, a 5 μL lipid precursor is first cast on the PVA gel film prepared above using a microsyringe. This quickly produces a lipid thin film upon solvent evaporation, which is further dried under vacuum overnight in the dark at room temperature. (4) Liposome production, which is carried out by hydrating the lipid films deposited on PVA gel with 1 mL of DI water at 45 °C for either 1 h (in the case of biotin-free liposomes) or 24 h (for liposomes containing 1 mol % biotin-DOPE). After a brief shake of the hydration cell housing the lipid deposits/gel/glass substrate, thus-produced liposomes are harvested with a pipette and stored at room temperature. An extended hydration period is found to be beneficial to the coalescence process of biotinylated Janus liposomes. All thus-formed liposomes are subsequently given 5−7 days to reach complete coalescence of their lipid domains before further use. Overall, PVA gels prepared from the two molecular weights are found to yield comparable liposome products.

Bioaffinity Assembly of Biotinylated Janus Liposomes. Binding between liposomes is initiated by mixing these biotin-decorated liposomes with NeutrAvidin at a mixing ratio of 5 (biotin) to 1 (protein), with the final biotin concentration typically held at ∼25 nM. The resulting mixture is briefly vortexed and then incubated at room temperature in the dark for durations specified in the main text.

Fluorescence Microscopy. Fluorescence images of giant liposomes were acquired on a Nikon A1+/MP confocal scanning laser microscope (Nikon Instruments, Inc., Melville, NY) using 10× objective and excitation laser lines at 488 and 561 nm. The corresponding green and red emission signals were filtered at 525 ± 25 and 595 ± 25 nm. For each measurement, a 10−15 μL liposome solution was first pipetted into a Poly(dimethylsiloxane) microwell reversibly sealed to a precleaned microscope cover slide (Corning No. 1, 22 × 22 mm, Corning, NY) and then given 1 h to settle under 100% humidity. Images of on-gel liposomes are obtained from an epifluorescence microscope (Nikon TE-2000 U, Japan) using 10× objective; filters used: excitation, 475 ± 20 nm, and emission, 561 nm long pass.

RESULTS AND DISCUSSION

We choose DPPC/DOPC/cholesterol ternary system for this investigation mainly because its liquid-ordered (l_o) and liquid-disordered (l_d) phase coexistence has been quantitatively mapped out and can be stably maintained at room temperature.[28−31] To form liposomes of this system, we have adopted

DOI: 10.1021/acs.langmuir.8b00798
Langmuir 2018, 34, 7509−7518

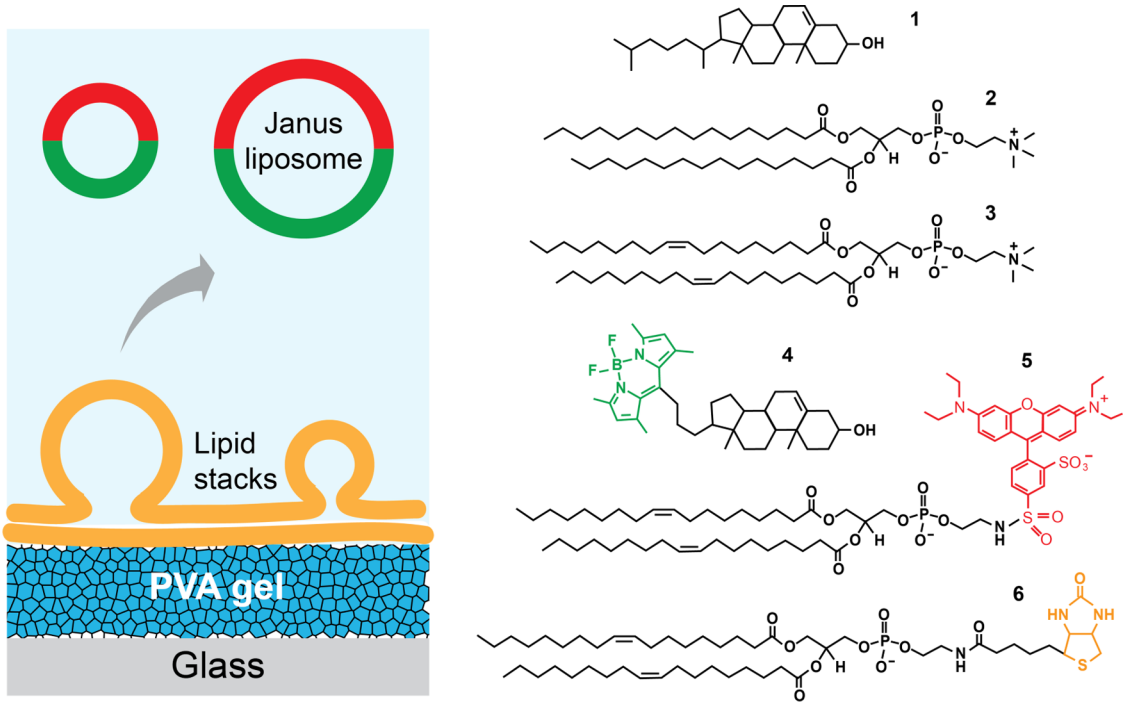

Figure 1. Formation of giant Janus liposomes via poly(vinyl alcohol) (PVA)-assisted lipid swelling. Left: schematic of the gel-assisted liposome formation process. Right: main lipids employed in this work (**1**–**6**): cholesterol, DPPC, DOPC, Bodipy-chol, rho-DOPE, and biotin-DOPE. Full names of these species are given in Experimental Section.

a protocol based on gel-assisted lipid swelling developed by Marques and co-workers[1] recently. Compared to passive supports, such as glass, the gel can provide active assistance to the hydration process in that its water-pulling gel matrix constantly drives water penetration along the direction perpendicular to the lipid stacks.[1] This greatly improves the liposome formation and detachment. As described in Experimental Section and illustrated in Figure 1, our procedure mainly features a hydration step, in which lipid stacks deposited on a dried PVA gel layer are soaked in water at 45 °C, which is above the phase-transition temperature of both DOPC and DPPC. Also included in the lipid precursors are 0.2 mol % Bodipy-labeled cholesterol (Bodipy-chol) and rhodamine-labeled DOPE (rho-DOPE), which are known to preferentially partition into the liquid-ordered[33] (l_o) and liquid-disordered[34] (l_d) phases, respectively, and serve as fluorescent lipid-phase indicators. Fluorescence imaging of the hydration process reveals fast production of high-quality liposomes, which form densely on the PVA gel and are largely free of other irregular lipid structures (Figure 2, top). A significant portion of liposomes tend to remain associated with each other and with the gel at the end of 1 h hydration, which can be easily suspended by briefly shaking the hydration cell. Only a low residual fluorescence can be observed from the gel layer after this process (Figure 2, bottom), which suggests a nearly complete removal of lipid deposits. Such high-yield liposome production has enabled us to routinely harvest these liposomes for subsequent uses. On the other hand, size analysis of >200 such liposomes from multiple batches shows a relatively wide distribution from a few to ∼40 μm (Figure 1, Supporting Information).

Confocal fluorescence microscopy further reveals that freshly prepared liposome samples only contain a small portion of liposomes with desired Janus geometry, that is, with their l_o/l_d phases separated completely into two hemispheres. By contrast, the majority of the liposomes initially display partial phase separation of some degree. Here, the predominant morphology features small circular l_d domains dispersed in a single, globally continuous l_o domain, while a small number of liposomes with stripe-shaped l_d/l_o domains are also observed (Figure 3). Such polymorphism reflects the kinetic mismatch between fast liposome formation and much slower domain coalescence within individual liposomes, allowing the latter process to be on full display while in transition. With respect to the energy landscape of lipid organization within individual liposomes, these morphologies correspond to the local energy minima. Complete coalescence of small lipid domains, which represents the global energy minimum of these liposomes, typically takes several days when stored at room temperature. Compared to this slow aging procedure, attempts to speed up the domain coalescence, for example, by overnight incubation of the harvested liposomes at 45 °C, only led to products of inconsistent quality. All liposomes presented in the rest of this work, therefore, have been first given 5–7 days to reach the intended Janus structure before further use, and the resultant Janus liposomes remain stable for at least several months.

Subsequent fluorescence measurements of these Janus liposomes in addition reveal that the majority of Janus liposomes formed within the same batch carry comparable l_o-to-l_d domain ratios. Such uniformity manifests another strength of this gel-assisted formation method and, moreover, presents us an opportunity to engineer the domain configuration in these liposomes through control of lipid composition. To test this possibility, we prepared three liposome samples containing the following DPPC/DOPC/cholesterol mixing ratios (mol %): 50:20:30, 35:35:30, and 30:50:20. All three compositions fall within the l_o/l_d-coexistence region in the phase diagram (area marked in green in Figure 4, top left) and are therefore

DOI: 10.1021/acs.langmuir.8b00798
Langmuir 2018, 34, 7509−7518

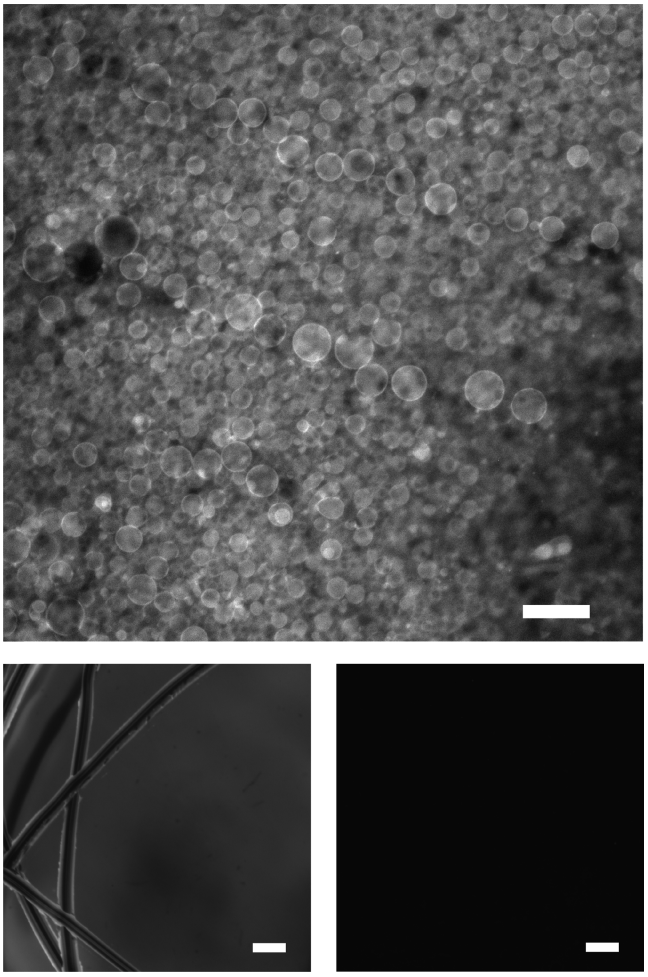

Figure 2. Fluorescence images of the gel-assisted Janus liposome production process. Top: fluorescence micrograph of Janus liposomes as they emerge from the PVA gel upon 1 h hydration. Bottom left: fluorescence micrograph of lipid stacks deposited on the PVA gel before hydration. The lipid/gel film was intentionally scratched by microtweezers to give contrast to the image. Bottom right: fluorescence micrograph of the same sample taken after hydration and liposome harvesting. Liposome composition (mol %): DPPC/DOPC/cholesterol/biotin-DOPE/rho-DOPE/Bodipy-chol = 35:35:30:1:0.2:0.2. Filters used: excitation, 475 ± 20 nm, and emission, 561 nm long pass. The scale bar is 100 μm.

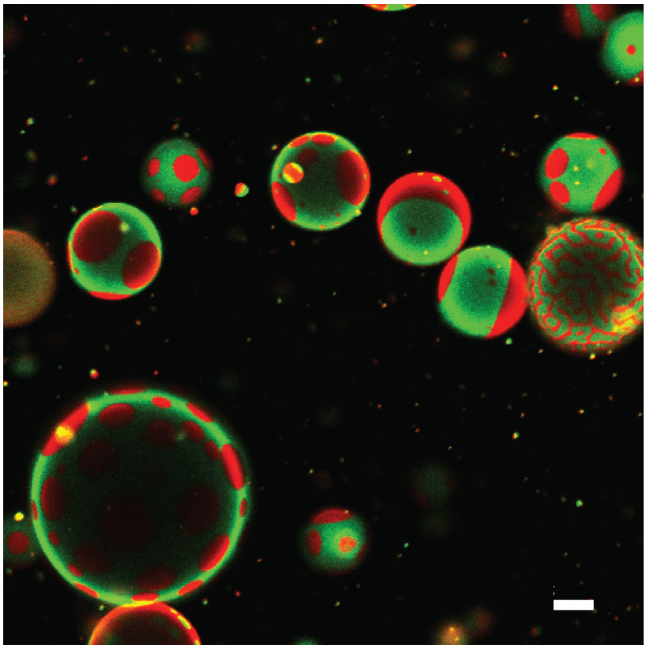

Figure 3. Confocal fluorescence micrograph of precursor Janus liposomes imaged 1 day after preparation. Liposome composition is the same as in Figure 2. The l_o and l_d domains are marked by Bodipy-chol (green fluorescence) and rho-DOPE (red fluorescence), respectively. The scale bar is 20 μm.

expected to yield Janus liposomes with minimized line tension across phase boundaries. Images shown in the rest of Figure 4 clearly confirm this projection and in addition identify a trend of transition in the relative domain size of these liposomes, going from l_d-minor (50:20:30) to roughly even-split (35:35:30) and then l_d-major (30:50:20) domain configurations. This trend is more quantitatively revealed by the Janus ratio, i.e., areal ratio of l_o to l_d domains, associated with these liposomes: l_d-minor (3.19 ± 1.57), even-split (0.92 ± 0.24), and l_d-major (0.39 ± 0.13) (Figure 2, Supporting Information). These results thus put us in position to start examining the influence of domain configuration on the interactions and assembling behavior of Janus liposomes.

To render these Janus liposomes surface-binding capability, we have looked into several phosphoethanolamine (PE) lipids with their amine headgroups conjugated to biotin. To realize biotin/avidin binding specific to liposome domains, we hypothesize that these biotin PE can be sorted into l_o (or l_d) domains according to their acyl chains, that is, DPPE into DPPC, or DOPE into DOPC. This requires a low biotin-PE doping level in liposomes so that its presence will not significantly impact the phase separation established by the three main lipid components. In this study, we have chosen to keep the biotin-PE doping level constant at 1 mol %. Also important is the potential reorganization/redistribution[35] of biotin-PE within the liposomes upon binding to avidin, which needs to be checked after liposome production.

Guided by these considerations, we have then found biotin-DOPE (**6**, Figure 1) to be a suitable biotin lipid conjugate for DPPC/DOPC/cholesterol Janus liposomes. As shown in Figure 5, high-quality liposomes displaying uniform phase separation can still be prepared when this lipid is included in the formation. Using a green-labeled avidin to bind these liposomes, moreover, we observe a strong colocalization between avidin and rho-DOPE, indicating that the incorporated biotin-DOPE almost exclusively resides in the l_d domains of these Janus liposomes. Importantly, this exclusive phase preference persists even when these biotinylated liposomes are challenged with high dosages of avidin, e.g., at 1:1 biotin/avidin mixing ratio. In comparison, for the other two lipids we briefly tested, biotin-cap-DOPE (l_d preferred) and biotin-cap-DPPE (l_o preferred), avidin binding could also be observed on the opposite domains, despite to a less extent than the preferred domains, when the avidin level was raised from 5:1 (biotin/avidin) to 1:1 (data not shown). The observed difference, first of all, illustrates the significant mechanical impact that multivalent biotin/avidin binding can impart on a fluid lipid membrane. Moreover, it suggests that lipid sorting, as exploited here, tends to work less effectively for lipids with more extended structures, which undermine the overall ordering/coordination among lipids in the lipid matrix and hence the strength of their association with certain domains.

DOI: 10.1021/acs.langmuir.8b00798
Langmuir 2018, 34, 7509−7518

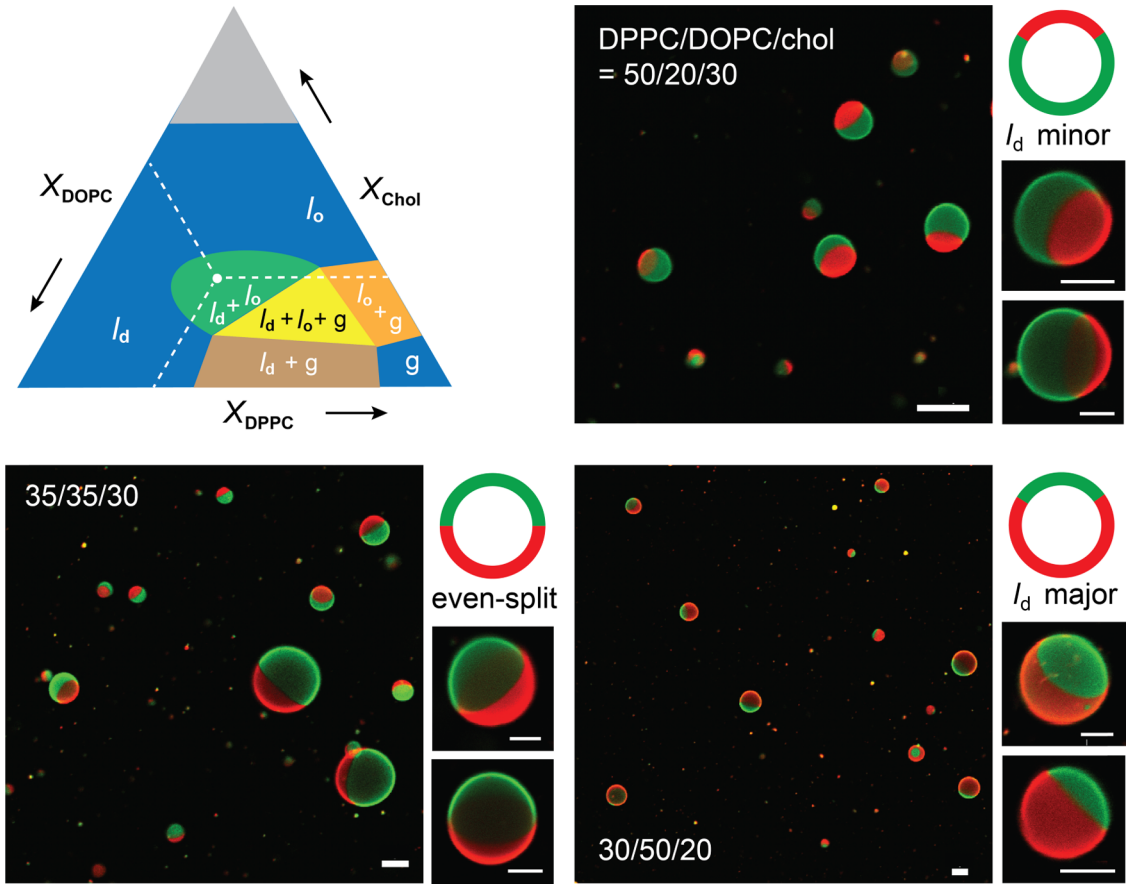

Figure 4. Janus liposomes with controlled domain configurations. Top left: a generic triangle phase diagram of DPPC/DOPC/cholesterol system at room temperature. Each point in the diagram represents a mixing ratio of the three components, whose fractions are specified by the three sides of the triangle. Different phases are color-coded, in which the three single-phase regions, liquid-ordered (l_o), liquid-disordered (l_d), and gel (g) phases, are shown in blue. The gray triangle at the top denotes lipid mixing ratios that do not lead to liposome formation. The three-phase-coexisting region ($l_o + l_d + g$, yellow) is surrounded by three two-phase-coexisting regions. More quantitative phase diagrams of this system can be found in refs 29 and 30. Top right and bottom: confocal fluorescence micrographs of Janus liposomes prepared from three DPPC/DOPC/cholesterol mixing ratios (in mol %). In each case, one large-area (scale bar: 20 μm) and two close-up (scale bar: 5 μm) images are presented. A cartoon drawing is also included in each case to indicate the expected domain configuration.

Bringing these findings together, we next examined the assembling behavior of biotinylated Janus liposomes carrying different domain configurations. Successful binding between liposomes is observed in all cases when they are incubated with avidin, which, as expected, occurs exclusively through l_d domains. Such formation, in addition, proceeds in a time-dependent fashion, producing first low populations of small liposome clusters among unbound individual liposomes and then aggregates that may engage more liposomes. Accordingly, we present these results in two parts below.

Summarized in Figure 6 are our main observations on the initial liposome cluster formation, taken after 2-day liposome/avidin incubation. For Janus liposomes with their binding l_d domain as the minor domain, dimer formation predominates (Figure 6a–c). The same also holds true for Janus liposomes with roughly equal l_o/l_d domains (Figure 6f–h). In either case, clusters with more than two members are only seen when there exists a significant size mismatch among binding partners such that small liposomes either fit into the grooves formed by large ones (Figure 6d,e) or co-bind a giant host (Figure 6i). In contrast, three-member clusters are routinely found to form alongside dimers for l_d-major Janus liposomes (Figure 6l–n vs 6j,k). Such disparity in assembling behavior most likely results from the larger portion of binding sites carried by l_d-major Janus liposomes, which not only increases the chance of successful binding upon liposomes' encounter, but also provides more room to accommodate multiliposome binding. Of the three types of liposomes tested, on the other hand, we observe no preferred angles or locations (e.g., cap vs phase boundary) for binding between l_d domains, suggesting uniform biotin distribution therein.

Another formation we have observed is the bulging of l_d domains in biotinylated Janus liposomes upon incubation with avidin, which, interestingly, occurs only in l_d-minor liposome samples (Figure 6c,d). Similar formation has been observed from phase-separated liposomes before, when these liposomes are subjected to certain physical perturbations,[27,36] e.g., temperature or osmotic pressure. According to the curvature elasticity model,[37−40] the shape of phase-separated liposomes at equilibrium is governed by the dynamic balance of two opposing forces: lipid bilayer bending vs line tension. The former originates from the curvature carried by the spherical liposome, whose departure from the ideally packed, planar bilayer configuration induces a mechanical stress across the entire liposome surface. Line tension, on the other hand, emanates from the size/chemical mismatch between lipids making up the phase boundary of the liposome, which scales linearly with the length of the boundary. These two oppose

DOI: 10.1021/acs.langmuir.8b00798
Langmuir 2018, 34, 7509−7518

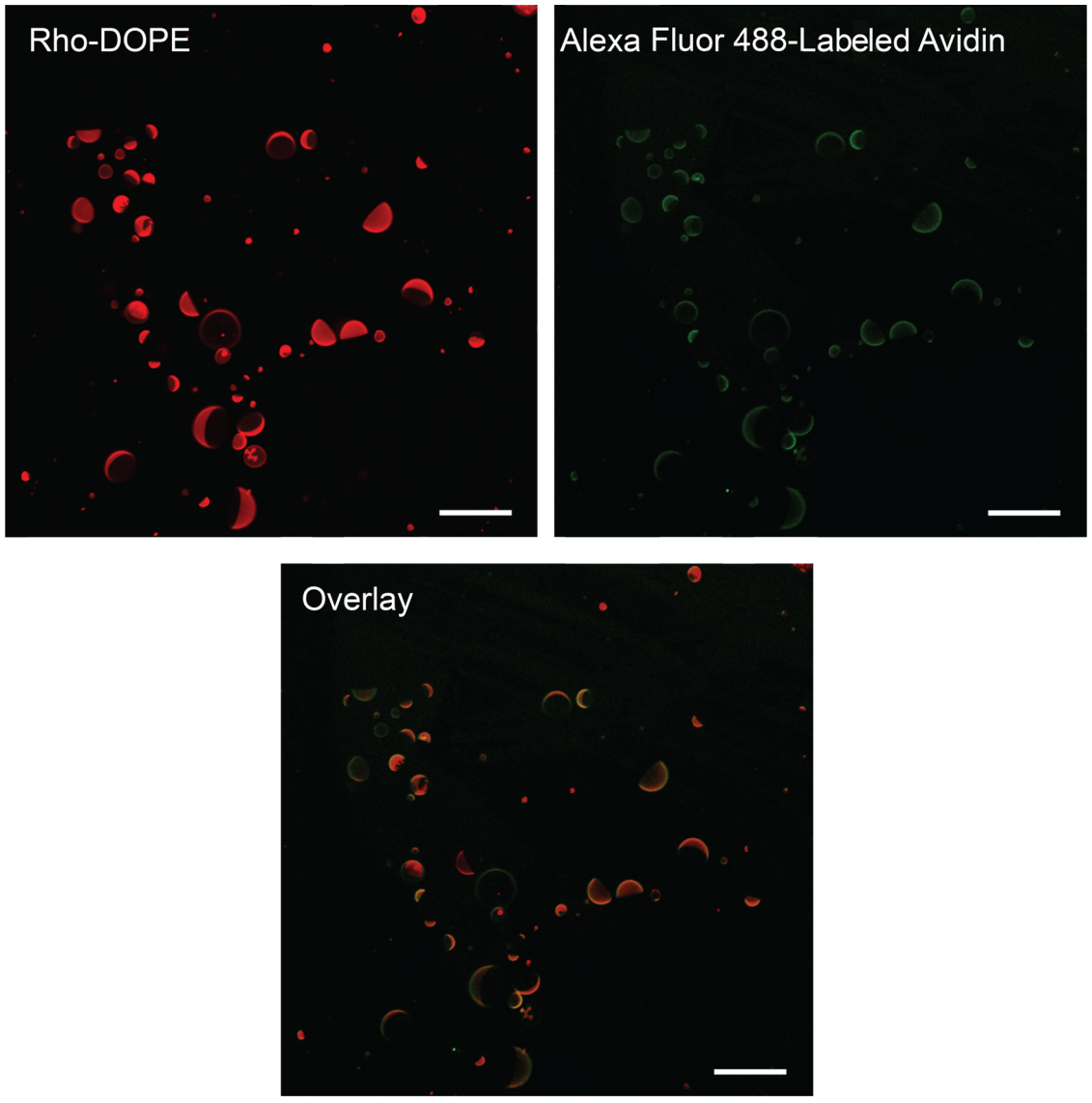

Figure 5. Phase preference of biotin-DOPE in DPPC/DOPC/cholesterol Janus liposomes. Top left: confocal fluorescence image of rho-DOPE displaying the l_d phase; the l_o domains are not labeled. Top right: green channel showing avidin location of the same liposome sample. Bottom: merged image displaying both red and green fluorescence. The scale bar is 50 μm.

each other in that the bending force intends to lower the liposome curvature, a process necessarily causing the phase boundary to expand, which line tension always acts to minimize (Figure 7). Thus-established shape equilibrium, moreover, is quite delicate in that the force balance is very susceptible to additional sources of perturbation that may arise in and around the liposome. Such perturbations include lipid lateral tension and osmotic pressure, which enter the equation by modifying the liposome area and volume, respectively (Figure 7). Complicating the phase transformation further is the different mechanical strength, or bending rigidity, built into different lipid domains. The l_o domains, comprising mainly DPPC and cholesterol, display a bending rigidity several times greater than that of the l_d domains[40] and thus are more resistant to a perturbation.

Considering its multibinding ability as well as added protein mass, avidin binding is expected to exert a significant perturbation to the organization/motion of biotin-DOPE within the l_d domains. This, in effect, raises the lateral tension of the outer l_d domains, which can drive liposome shape transformation. Because bulging produces more curved l_d domains that can directly offset the lateral tension increase, it stands as a thermodynamically favored transformation pathway. On the other hand, two factors may account for its exclusive occurrence in l_d-minor liposomes. First is in the membrane mechanics. Compared to Janus liposomes with even-split domains, l_d-minor liposomes have smaller phase boundaries, which produce lower line tensions and thus less resistance to shape transformation. Similar argument also holds true for the l_o-minor liposomes, whose bulging would require significant binding of the l_o domains, an unlikely event considering their higher bending rigidity and lack of local perturbation, i.e., avidin binding. Second, assuming exclusive biotin-DOPE partitioning into the l_d domains, its effective concentration should be the highest in the l_d-minor liposomes (due to the same 1% being concentrated into a smaller area of liposomes). This can lead to a denser avidin binding and hence a stronger perturbation.

Finally, we examined the clustering of biotinylated Janus liposomes at longer avidin incubation times. For l_d-minor liposomes, dimers and trimers remain the most common

DOI: 10.1021/acs.langmuir.8b00798
Langmuir 2018, 34, 7509−7518

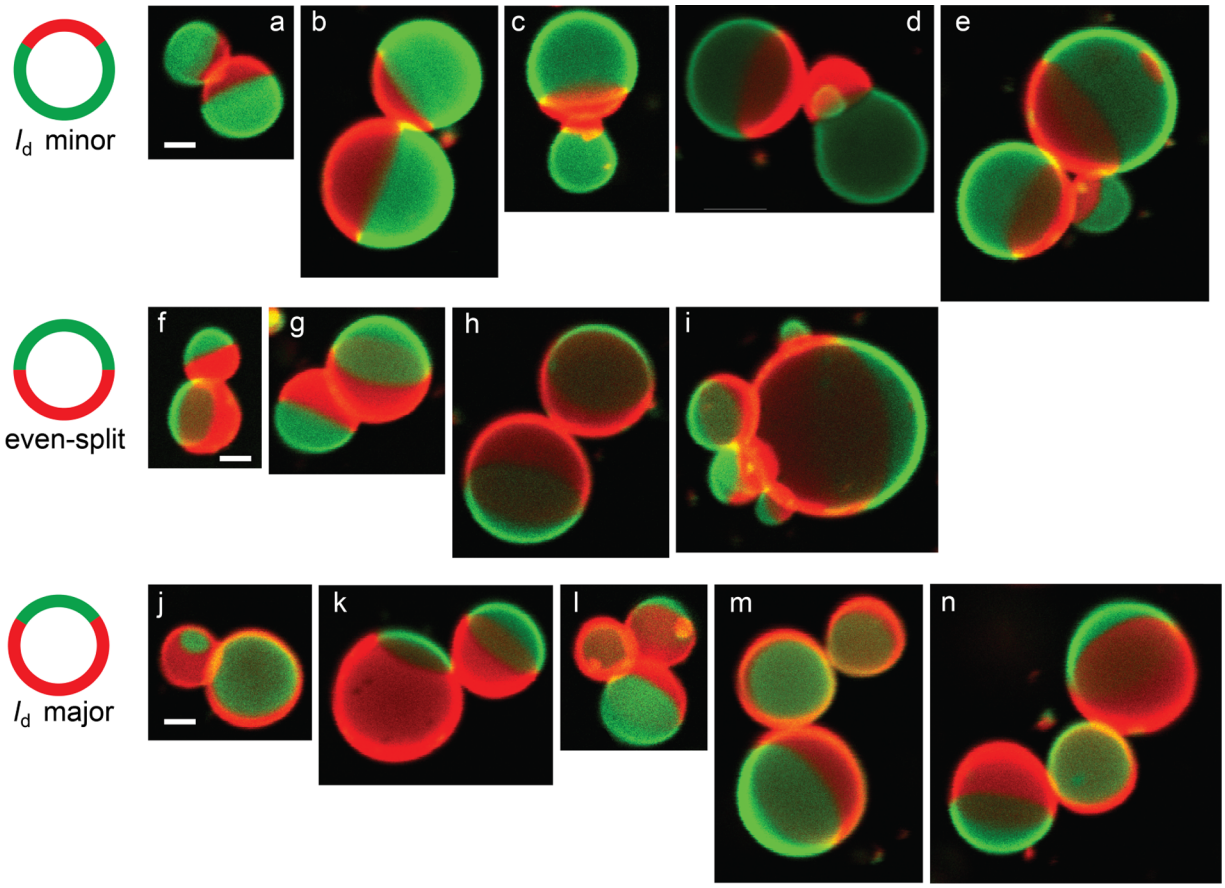

Figure 6. Clustering of biotin-decorated Janus liposomes upon incubation with avidin. Confocal fluorescence images of these clusters are presented in three rows according to liposome domain configuration. DPPC/DOPC/cholesterol mixing ratios (in mol %): l_d-minor, 50:20:30; even-split, 35:35:30; and l_d-major, 30:50:20. All liposomes, in addition, contain 1% biotin-DOPE and 0.2% rho-DOPE and Bodipy-chol. Scale bars represent 5 μm and apply to all images.

clusters formed after 7 days, which is likely due to their relatively small binding domains spatially limiting further growth of the seed clusters, as discussed earlier. Larger clusters were only occasionally found, and one of such, a tetramer, is shown in Figure 8, left. Compared to clusters obtained after 2-day incubation, a distinct feature here is the significantly larger areas of contact between l_d domains. This clearly results from the extended incubation, which enables avidin to continue to arrive at the interface and cross-link the remaining l_d domains between binding liposomes. In the case of l_d-major liposomes, larger clusters containing 5−7 members are routinely observed after 7 days (Figure 8, right), confirming the capability of their larger biotin-occupying domains to promote further liposome binding. Similar to l_d-minor liposomes, diaphragms form between contacting liposomes, which are accompanied by minor lipid exchange between l_o and l_d domains, as evident from the resultant yellow fluorescence. In marked contrast to these two cases, much larger liposome aggregates often consisting of dozens of binding members are consistently found to form for even-split Janus liposomes when similarly treated (Figure 8, middle). In each of these aggregates, we also observe substantial lipid interfusion, which appears to occur both within individual liposomes and between neighboring liposomes. This exclusive formation tends to reoccur when these liposomes are tested at different concentrations or biotin/avidin mixing ratios (data not shown).

We believe that this intriguing behavior of even-split liposomes results from a cascade of effects. It starts with their even-split geometry, which places the l_o/l_d phase boundary near the liposome equator, the longest one of the three. This means that, on average, these even-split liposomes bear the largest line tension, which scales linearly with the length of the phase boundary. Such high built-in tension makes these even-split liposomes more susceptible to external perturbations. Geometry also makes another critical difference when an unbound even-split liposome approaches an existing liposome cluster—it provides the newcomer maximal chance to contact the cluster on the opposite domains (Figure 8, middle, inset). In comparison, such access is significantly compromised in the other two types of liposomes, whose major domains dominate their interactions (Figure 8, left/right, insets). Establishing contacts between opposite domains is critical, simply because it triggers cross-phase lipid exchange. While such lipid exchange can only occur along the phase boundary in individual liposomes, a largely one-dimensional process, the same process takes place across the entire contacting surfaces between liposomes and thus is expected to be more efficient. A direct outcome of such lipid exchange is the homogenization of biotin, which enables global avidin binding and hence continual growth of the seed clusters in an uncontrolled manner, analogous to homogenous liposome aggregation.[32,41] This eventually leads to the formation of large aggregates. Taken together, this mechanism may be summarized as follows:

DOI: 10.1021/acs.langmuir.8b00798
Langmuir 2018, 34, 7509−7518

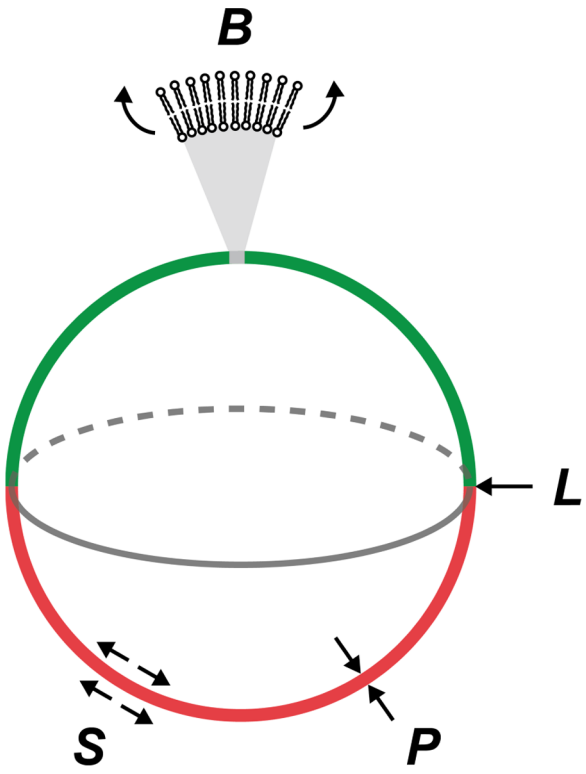

Figure 7. Main forces that govern the shape and shape transformation of biphasic liposomes according to the curvature elasticity model. B, lipid-bending force; L, line tension; S, lateral surface tension; P, osmotic pressure. Except for line tension, which operates on and around the phase boundary (circle in gray), all other forces act across the whole surface/body of the liposome.

geometry → high susceptibility/access → lipid exchange → biotin homogenization → global binding → aggregation. To put this mechanism on a firm footing, further work is clearly needed.

CONCLUSIONS AND OUTLOOK

Motivated by the technical promises of Janus liposomes as well as the lack of general methods to synthesize such asymmetrical lipid colloids, we have developed in this work a high-yield procedure for preparing microsized Janus liposomes via gel-assisted lipid swelling. Since this method exploits general lipid-organizing principles to form the liposomes, it is expected to be applicable to other types of phase-separating lipid systems. This method is also precise, enabling Janus liposomes of specific domain configurations to be reliably made, which, to our knowledge, have not been demonstrated before. The versatility of this method is further demonstrated by its ability to afford straightforward incorporation of biotin-conjugated lipids into the formation, which produces Janus liposomes with asymmetrical, domain-specific affinity binding ability. Finally, we have carefully monitored and interpreted the domain-specific cluster/aggregate formation of these Janus liposomes. Along this direction, research is currently ongoing in our laboratory to further increase the complexity of these Janus liposomes, for example, by exploiting charged and other lipids carrying additional functionalities.

Findings of this work may be of interest to researchers in several areas. (1) Patchy particles. With a reliable preparation method in hand, it is now feasible to test these Janus liposomes alongside their inorganic/polymer cousins as building blocks and motors. Understanding the physicochemical similarities and differences between various types of patchy particles, for one, will help us design better applications according to their strengths. (2) Bioanalytical/biomedical applications. A good number of homogenous/heterogeneous biodetection schemes have been developed using symmetrical liposomes,[42] taking advantage of their aqueous core and soft, modifiable surfaces combined in a small package. While Janus liposomes are expected to work equally well in many of these bioassays, a more interesting question to entertain here is: How to take advantage of the phase separation and broken symmetry of Janus liposomes to design new applications beyond current liposome biotechnology. For example, by adding a second binding functionality into the l_o phase of our biotinylated Janus liposomes, a bifunctional liposome system may be easily envisioned. (3) Membrane biophysics. The majority of phase-separated liposomes that have appeared in the biophysical literature are prepared using electroformation, which is known to suffer several limitations, such as potential lipid damage and biases toward charged lipids. In this regard, the field can clearly benefit from having a robust alternative. On the other hand, our

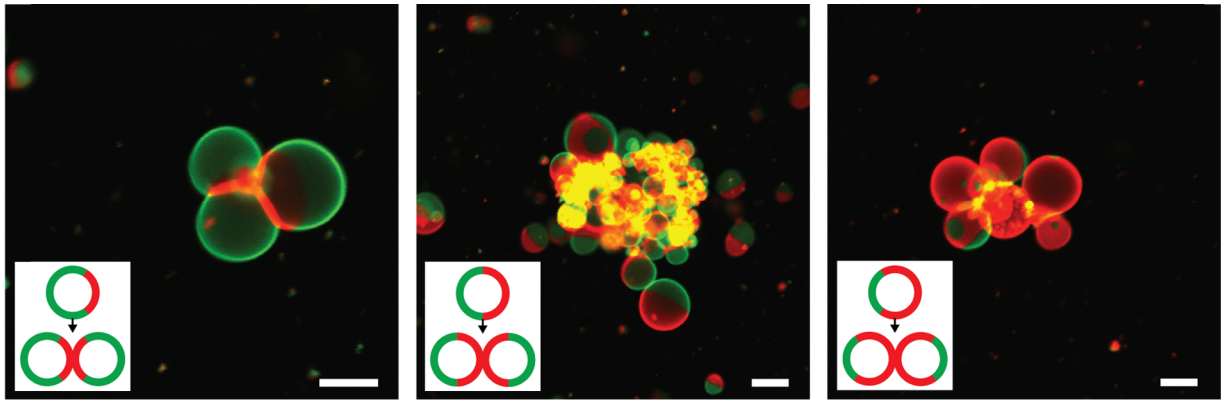

Figure 8. Aggregation and lipid fusion of biotin-decorated Janus liposomes upon extended (typically 1 week) incubation with avidin. DPPC/DOPC/cholesterol mixing ratios (from left to right): l_d-minor, 50:20:30; even-split, 35:35:30; and l_d-major, 30:50:20. All liposomes, in addition, contain 1% biotin-DOPE and 0.2% rho-DOPE and Bodipy-chol. The scale bar is 20 μm. Drawings embedded in the images illustrate a comparable clustering scenario for the three types of liposomes, in which a free liposome approaches a symmetrically bound liposome dimer from the top in an identical manner.

DOI: 10.1021/acs.langmuir.8b00798
Langmuir 2018, 34, 7509−7518

results point to the possibility of inducing liposome shape transformation by protein adhesion and moreover the importance of liposome domain configuration and mechanical properties leading to such changes. This may be further developed into a model system for studying lipid bulging/budding, a fundamental process essential to many biological functions.[43,44]

■ ASSOCIATED CONTENT

Supporting Information

The Supporting Information is available free of charge on the ACS Publications website at DOI: 10.1021/acs.langmuir.8b00798.

Statistical analysis plots on liposome size distribution and domain configuration (PDF)

■ AUTHOR INFORMATION

Corresponding Author

*E-mail: wzz0001@auburn.edu.

ORCID

Wei Zhan: 0000-0001-7096-9261

Author Contributions

†M.W. and Z.L. contributed equally to this work.

Notes

The authors declare no competing financial interest.

■ REFERENCES

(1) Weinberger, A.; Tsai, F.-C.; Koenderink, G.; Schmidt, T. F.; Itri, R.; Meier, W.; Schmatko, T.; Schoder, A.; Marques, C. Gel-Assisted Formation of Giant Unilamellar Vesicles. *Biophys. J.* **2013**, *105*, 154−164.

(2) Jiang, S.; Chen, Q.; Tripathy, M.; Luijten, E.; Schweizer, K. S.; Granick, S. Janus Particle Synthesis and Assembly. *Adv. Mater.* **2010**, *22*, 1060−1071.

(3) Walther, A.; Müller, A. H. E. Janus Particles: Synthesis, Self-Assembly, Physical Properties, and Applications. *Chem. Rev.* **2013**, *113*, 5194−5261.

(4) Pang, X.; Wan, C.; Wang, M.; Lin, Z. Strictly Biphasic Soft and Hard Janus Structures: Synthesis, Properties, and Applications. *Angew. Chem., Int. Ed.* **2014**, *53*, 5524−5538.

(5) Lehtonen, J. Y.; Holopainen, J. M.; Kinnunen, P. K. J. Evidence for the Formation of Microdomains in Liquid Crystalline Large Unilamellar Vesicles Caused by Hydrophobic Mismatch of the Constituent Phospholipids. *Biophys. J.* **1996**, *70*, 1753−1760.

(6) Almeida, P. F. F.; Pokorny, A.; Hinderliter, A. Thermodynamics of Membrane Domains. *Biochim. Biophys. Acta, Biomembr.* **2005**, *1720*, 1−13.

(7) Ohvo-Rekilä, H.; Ramstedt, B.; Leppimäki, P.; Slotte, J. P. Cholesterol Interactions with Phospholipids in Membranes. *Prog. Lipid Res.* **2002**, *41*, 66−97.

(8) Róg, T.; Pasenkiewicz-Gierula, M.; Vattulainen, I.; Karttunen, M. Ordering Effects of Cholesterol and Its Analogues. *Biochim. Biophys. Acta* **2009**, *1788*, 97−121.

(9) New, R. R. C. *Liposome: A Practical Approach*; Oxford University Press: Oxford, U.K., 1990.

(10) Lasic, D. D. Novel Applications of Liposomes. *Trends Biotechnol.* **1998**, *16*, 307−321.

(11) Collier, J. H.; Messersmith, P. B. Phospholipid Strategies in Biomineralization and Biomaterials Research. *Annu. Rev. Mater. Res.* **2001**, *31*, 237−263.

(12) Gibbs, B. F.; Kermasha, S.; Alli, I.; Mulligan, C. N. Encapsulation in the Food Industry: a Review. *Int. J. Food Sci. Nutr.* **1999**, *50*, 213−224.

(13) Nohynek, G. J.; Lademann, J.; Ribaud, C.; Roberts, M. S. Grey Goo on the Skin? Nanotechnology, Cosmetic and Sunscreen Safety. *Crit. Rev. Toxicol.* **2007**, *37*, 251−277.

(14) Chang, H.-I.; Yeh, M.-K. Clinical Development of Liposome-Based Drugs: Formulation, Characterization, and Therapeutic Efficacy. *Int. J. Nanomed.* **2012**, *7*, 49−60.

(15) Bangham, A. D. Physical Structure and Behavior of Lipids and Lipid Enzymes. *Adv. Lipid Res.* **1963**, *1*, 65−104.

(16) Du, J.; O'Reilly, R. K. Anisotropic Particles with Patchy, Multicompartment and Janus Architectures: Preparation and Application. *Chem. Soc. Rev.* **2011**, *40*, 2402−2416.

(17) Loget, G.; Kuhn, A. Bulk Synthesis of Janus Objects and Asymmetric Patchy Particles. *J. Mater. Chem.* **2012**, *22*, 15457−15474.

(18) Hong, L.; Cacciuto, A.; Luijten, E.; Granick, S. Clusters of Charged Janus Spheres. *Nano Lett.* **2006**, *6*, 2510−2514.

(19) Evers, C. H. J.; Luiken, J. A.; Bolhuis, P. G.; Kegel, W. K. Self-Assembly of Microcapsules via Colloidal Bond Hybridization and Anisotropy. *Nature* **2016**, *534*, 364−368.

(20) Jiang, H.-R.; Yoshinaga, N.; Sano, M. Active Motion of a Janus Particle by Self-Thermophoresis in a Defocused Laser Beam. *Phys. Rev. Lett.* **2010**, *105*, No. 268302.

(21) Ma, X.; Jannasch, A.; Albrecht, U.-R.; Hahn, K.; Miguel-López, A.; Schäffer, E.; Sánchez, S. Enzyme-Powered Hollow Mesoporous Janus Nanomotors. *Nano Lett.* **2015**, *15*, 7043−7050.

(22) Radhakrishnan, A.; McConnell, H. M. Condensed Complexes of Cholesterol and Phospholipids. *Biophys. J.* **1999**, *77*, 1507−1517.

(23) McConnell, H. M.; Vrljic, M. Liquid-Liquid Immiscibility in Membranes. *Annu. Rev. Biophys. Biomol. Struct.* **2003**, *32*, 469−492.

(24) Feigenson, G. W. Phase Boundaries and Biological Membranes. *Annu. Rev. Biophys. Biomol. Struct.* **2007**, *36*, 63−77.

(25) Dietrich, C.; Bagatolli, L. A.; Volovyk, Z. N.; Thompson, N. L.; Levi, M.; Jacobson, K.; Gratton, E. Lipid Rafts Reconstituted in Model Membranes. *Biophys. J.* **2001**, *80*, 1417−1428.

(26) Samsonov, A. V.; Mihalyov, I.; Cohen, F. S. Characterization of Cholesterol-Sphingomyelin Domains and Their Dynamics in Bilayer Membranes. *Biophys. J.* **2001**, *81*, 1486−1500.

(27) Veatch, S. L.; Keller, S. L. Separation of Liquid Phases in Giant Vesicles of Ternary Mixtures of Phospholipids and Cholesterol. *Biophys. J.* **2003**, *85*, 3074−3083.

(28) Veatch, S. L.; Polozov, I. V.; Gawrisch, K.; Keller, S. L. Liquid Domains in Vesicles Investigated by NMR and Fluorescence Microscopy. *Biophys. J.* **2004**, *86*, 2910−2922.

(29) Veatch, S. L.; Soubias, O.; Keller, S. L.; Gawrisch, K. Critical Fluctuations in Domain-Forming Lipid Mixtures. *Proc. Natl. Acad. Sci. U.S.A.* **2007**, *104*, 17650−17655.

(30) Davis, J. H.; Clair, J. J.; Juhasz, J. Phase Equilibria in DOPC/DPPC-d_{62}/Cholesterol Mixtures. *Biophys. J.* **2009**, *96*, 521−539.

(31) Juhasz, J.; Sharom, F. J.; Davis, J. H. Quantitative Characterization of Coexisting Phases In DOPC/DPPC/Cholesterol Mixtures: Comparing Confocal Fluorescence Microscopy and Deuterium Nuclear Magnetic Resonance. *Biochim. Biophys. Acta* **2009**, *1788*, 2541−2552.

(32) Beales, P. A.; Nam, J.; Vanderlick, T. K. Specific Adhesion between DNA-Functionalized "Janus" Vesicles: Size-Limited Clusters. *Soft Matter* **2011**, *7*, 1747−1755.

(33) Ariola, F. S.; Li, Z.; Cornejo, C.; Bittman, R.; Heikal, A. A. Membrane Fluidity and Lipid Order in Ternary Giant Unilamellar Vesicles Using a New Bodipy-Cholesterol Derivative. *Biophys. J.* **2009**, *96*, 2696−2708.

(34) Gudheti, M. V.; Mlodzianoski, M.; Hess, S. T. Imaging and Shape Analysis of GUVs as Model Plasma Membranes: Effect of Trans DOPC on Membrane Properties. *Biophys. J.* **2007**, *93*, 2011−2023.

(35) Manley, S.; Horton, M. R.; Lecszynski, S.; Gast, A. P. Sorting of Streptavidin Protein Coats on Phase-Separating Model Membranes. *Biophys. J.* **2008**, *95*, 2301−2307.

(36) Baumgart, T.; Hess, S. T.; Webb, W. W. Imaging Coexisting Fluid Domains in Biomembrane Models Coupling Curvature and Line Tension. *Nature* **2003**, *425*, 821−824.

DOI: 10.1021/acs.langmuir.8b00798
Langmuir 2018, 34, 7509−7518

(37) Helfrich, W. Elastic Properties of Lipid Bilayers: Theory and Possible Experiments. *Z. Naturforsch., C* **1973**, *28*, 693−703.
(38) Jülicher, F.; Lipowsky, R. Domain-Induced Budding of Vesicles. *Phys. Rev. Lett.* **1993**, *70*, 2964−2967.
(39) Seifert, U. Configurations of Fluid Membranes and Vesicles. *Adv. Phys.* **1997**, *46*, 13−137.
(40) Baumgart, T.; Das, S.; Webb, W. W.; Jenkins, J. T. Membrane Elasticity in Giant Vesicles with Fluid Phase Coexistence. *Biophys. J.* **2005**, *89*, 1067−1080.
(41) Kisak, E. T.; Kennedy, M. T.; Trommeshauser, D.; Zasadzinski, J. A. Self-Limiting Aggregation by Controlled Ligand-Receptor Stoichiometry. *Langmuir* **2000**, *16*, 2825−2831.
(42) Edwards, K. A.; Baeumner, A. J. Liposomes in Analyses. *Talanta* **2006**, *68*, 1421−1431.
(43) Bonifacino, J. S.; Glick, B. S. The Mechanisms of Vesicle Budding and Fusion. *Cell* **2004**, *116*, 153−166.
(44) Zimmerberg, J.; Kozlov, M. M. How Proteins Produce Cellular Membrane Curvature. *Nat. Rev. Mol. Cell Biol.* **2006**, *7*, 9−19.

DOI: 10.1021/acs.langmuir.8b00798
Langmuir 2018, 34, 7509−7518